Available online at www.sciencedirect.com
SCIENCE DIRECT®
Journal of Molecular Catalysis A: Chemical 220 (2004) 167–182
JOURNAL OF MOLECULAR CATALYSIS A: CHEMICAL
www.elsevier.com/locate/molcata

Kinetics and mechanism of the hydroformylation of styrene catalysed by the rhodium/TPP system (TPP = 1,2,5-triphenyl-1*H*-phosphole)

C. Bergounhou*, D. Neibecker, R. Mathieu

Laboratoire de Chimie de Coordination du CNRS, 205 Route de Narbonne, 31077 Toulouse Cedex 4, France

Received 20 June 2003; received in revised form 7 June 2004; accepted 11 June 2004

Abstract

The kinetic study of the hydroformylation of styrene catalysed by the rhodium/1,3,5-triphenyl-1*H*-phosphole (TPP) system has been facilitated by the fact that a catalytic system having two TPP ligands per Rh atom is maintained all along the catalytic cycle and no dissociation of a TPP ligand has to be considered during this cycle. This has allowed us to propose a model of mechanism with an association complex between the styrene and the unsaturated $HRh(CO)(TPP)_2$ species. An analytical equation of the reaction rate has been established which acceptably characterises the behaviour of the reaction rate according to the concentration of the various species. This study reveals that the selectivity between linear and branched alkyl-rhodium is under thermodynamic control and the reversibility of the transformation of the alkyl into acyl-rhodium isomers has not clearly been established but suggested by the observations. An inhibiting effect of the produced aldehydes, through complexation with rhodium has also been put in evidence. This study emphasizes also the complex role of the CO and H_2 partial pressures on the rate of reaction. A single catalytic cycle, only differentiated by the formation of linear or branched aldehydes, based on these observations and consistent with the kinetic equation is proposed.

Keywords: Hydroformylation; Kinetics; Mechanism; Rhodium; 1,2,5-Triphenyl-1*H*-phosphole; Styrene

1. Introduction

With a world-wide production of several million tons a year, the hydroformylation of olefins is one of the main industrial reaction carried out by homogeneous catalysis [1]. Rhodium–phosphine based catalysts operate at lower temperature than earlier cobalt based catalysts and now represent the most used catalyst systems for this reaction.

In parallel to studies of the optimisation of reaction conditions and catalytic systems, numerous mechanistic studies were conducted [2] on the rhodium/phosphane systems [3,4]. Most of the published results concern the rhodium–triphenylphosphine catalysts used in the industrial plants for the hydroformylation of propene [1]. Some intermediate complexes in the catalytic cycle were isolated or modelled [5–7], and numerous experiments proved very useful for a better understanding of the reaction mechanism [8,9].[1] However, some steps are not completely demonstrated.

Pioneering studies by Wilkinson and co-workers [10] in 1968 led to the proposal of a first mechanism based on two competitive pathways, namely, a dissociative pathway and an associative one (today almost neglected). The proposal of a dissociative pathway is reminiscent to that of the hydroformylation with cobalt catalysts, first established by Heck and Breslow [11]. In such a scheme, the hydride complex $HRh(CO)_2(PPh_3)_2$ is formed whatever is the rhodium source, but the nature of the active species was often the object of controversy. For instance, in the initially proposed mechanism, the unsaturated species $HRh(CO)_2(PPh_3)$ was considered. However, in 1970, Brown and Wilkinson [12] suggested a second dissociative way leading to the active species $HRh(CO)(PPh_3)_2$ [13,14] (Fig. 1).

* Corresponding author. Tel.: +335-61-33-3168; fax: +335-61-55-3003.
E-mail address: bergounh@lcc-toulouse.fr (C. Bergounhou).

[1] Representative experimental data on our complexes (NMR, IR) are printed in paragraph 4.5 (Section 4). A full paper including in particular their characterisation is in preparation.

1381-1169/$ – see front matter © 2004 Elsevier B.V. All rights reserved.
doi:10.1016/j.molcata.2004.06.008

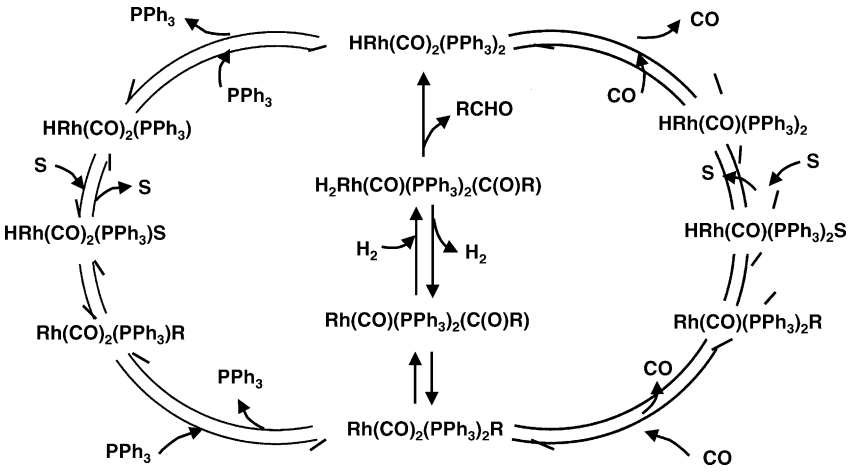

Fig. 1. Hydroformylation mechanism: carbonyl and phosphine dissociative pathway (S = substratum; R = linear or branched alkyl group).

The latter hypothesis was adapted later by several authors using other ligands [15–17]. It was confirmed for triphenylphosphine by in situ IR studies of Moser et al. [18] suggesting that complex $HRh(CO)(PPh_3)_2$ is involved in the main catalytic cycle. However, Unruh and Christenson [19] showed that a species containing three phosphane ligands could be active in hydroformylation catalysed by rhodium. This observation was recently confirmed by Bianchini et al. [20]. On the contrary, van Leeuwen and co-workers [21] showed that a rhodium complex with an encumbered phosphite, was involved in the catalytic cycle with only one of the phosphite ligand bound to rhodium.

Another subject of controversy is the nature of the rate-determining step. Evans et al. [10] suggested that oxidative addition of H_2 to the acyl-rhodium complex is the rate-determining step but Moser et al. [18] proposed the formation of the complex $HRh(CO)(PPh_3)_2$, by CO's dissociation from $HRh(CO)_2(PPh_3)_2$. To explain the influence of the CO/H_2 ratio on the linear/branched aldehyde ratio, Unruh and Christenson [19] suggested that the H_2 activation is the rate-determining step of the catalytic cycle leading to the linear aldehyde and that the formation of the alkyl-rhodium complex is the rate-determining step of the cycle leading to the branched aldehyde. More recently, van Rooy et al. [22] and van der Veen et al. [23] attributed the rate-determining step to the coordination or/and the insertion of a terminal alkene into the Rh–H bond.

Numerous kinetic studies were carried out to clarify the mechanism of the hydroformylation catalysed by rhodium–phosphane complexes [10,15,24–28], but they are not generally satisfactory because the range of reaction conditions is limited, the partial orders are often fractional, the linear aldehyde selectivity changes with the reaction parameters. As a consequence, the kinetic law is too complex to draw definite conclusions with regard to the reaction mechanism.

Despite this complexity, these studies have revealed two important parameters, the Rh/P ratio and the phosphane properties. The Rh/P ratio governs the formula of the complex involved in the catalytic cycle and its variation leads to the modulation of the catalytic activity and selectivity. As a consequence, when the hydroformylation reaction is carried out with complexes for which the Rh/P ratio is held constant throughout the catalytic cycle, the mechanism is strongly simplified and becomes an ideal case for a kinetic study [16,17].

Some years ago, Réau [29] checked a series of phospholes for the hydroformylation of different olefins [30–33]. The ligand 1,2,5-triphenyl-1*H*-phosphole (TPP) was the most active under very smooth temperature and pressure conditions (25–80 °C; 20–30 bar). Preliminary kinetic studies for the hydroformylation of styrene revealed the remarkable characteristics of this system [34]: its catalytic activity is systematically greater than the equivalent Rh/PPh_3 system [29] and is constant as soon as the Rh/TPP ratio is superior or equal to 2. The aldehyde chemoselectivity is 100% (2-phenylpropanal and 3-phenylpropanal) and the linear and branched aldehyde selectivity is roughly constant. The study of the influence of the Rh/TPP ratio in the case of hex-1-ene [30,31] and styrene [35] revealed the same behaviour.

Polo et al. [36] too, observed a significantly constant catalytic activity at various Rh/TPP ratio for the hydroformylation of 2,3-dihydrofurane and 2,5-dihydrofurane. It could thus be concluded that contrary to the Rh/PPh_3 systems, the Rh/TPP system leads to an active species with only two ligands TPP [35,37].

The results of our preliminary kinetic studies [34] allowed us to propose the following equation rate:

$$R = -\frac{\mathrm{d}[\text{styrene}]}{\mathrm{d}t} = 0.099[\text{styrene}]_0^{-0.47}[\text{styrene}]^1[\text{precursor}]^1\left[\frac{p\mathrm{H_2}}{p\mathrm{CO}}\right]^1$$

In the absence of a detailed study of the possible catalytic intermediates, it was difficult to rationalise the styrene

fractional order. We, therefore, undertook a more detailed study of the catalytic system along two complementary directions:

- The identification and study of the properties of the organometallics complexes (reaction intermediates) formed in the reaction mixtures.
- The conduction of additional kinetics experiments and the improvement of the kinetic studies by introduction of a new program for data acquisition and treatment.

In this paper, we present our conclusions about the reaction mechanism of the hydroformylation of styrene catalysed by the Rh/TPP system, based mainly on kinetic measurements and with the help of spectroscopic studies which will be fully presented in a separate paper.

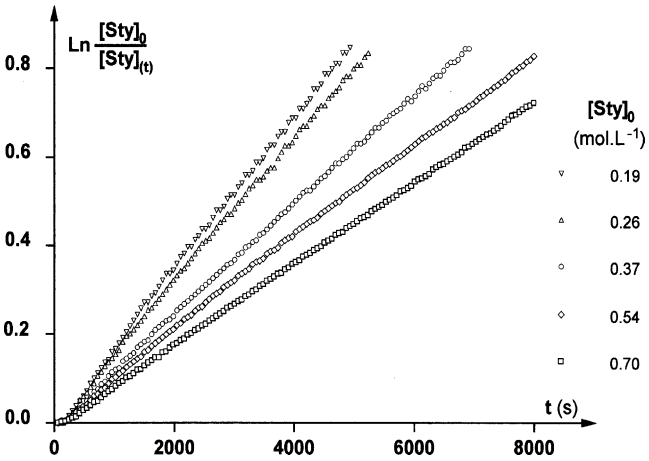

Fig. 2. Styrene order determination (different styrene concentrations).

2. Results and discussion

Kinetic experiments were carried out by the method of constant initial concentrations: each variable was studied separately, all the other experimental parameters being equal in other respects. These conditions allowed to calculate the rate at the origin of times and the average rate constant of the reaction. The experimental conditions and the calculated values are collected in Table 1.

2.1. Kinetic study of the influence of the various parameters of the reaction

2.1.1. Study of the influence of the styrene concentration (experiments 1–5)

Application of the integral method to all the data points leads to plot $\ln([\mathrm{Sty}]_0/[\mathrm{Sty}]_{(t)}) = f(t)$ for the five experiments with different initial styrene concentrations (Fig. 2). The plotted curves appear as straight lines, consistent with a current styrene order equal to 1. However, they are not superimposed, do not pass by the origin of axes and a weak non-linearity can be discerned for conversions lower than 40% ($(\ln([\mathrm{Sty}]_0/[\mathrm{Sty}]_{(t)}) < 0.5$). The $k_{1\mathrm{obs}}$ value calculated from the average slope of the straight line confirms a value of -0.47 for the initial styrene order.

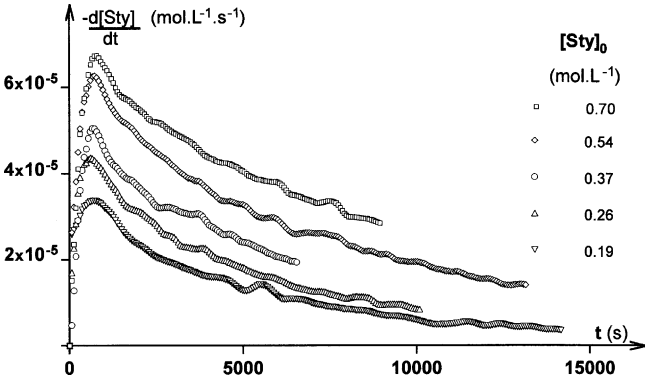

Fig. 3. Reaction rate vs. time (different styrene concentrations).

The graph $R_{(t)} = f(t)$, for the various initial styrene concentrations (Fig. 3), shows at least two phases in the reaction progress.

Table 1
Experiments used for the calculation of the rate constant ($t = 40\,^{\circ}\mathrm{C}$)

Run	$[\mathrm{Sty}]_0$ (mol L^{-1})	[Prec] (mol L^{-1})	P_{total} (bar)	$P_{\mathrm{H_2}}/P_{\mathrm{CO}}$	R_0 (mol L^{-1} s^{-1})	k_{obs} (s^{-1})	Branched/linear[a]	K_{vit} (mol L^{-1})$^{-0.53}$ s^{-1})
1	0.70	8.0×10^{-4}	20	1	6.65×10^{-5}	0.95×10^{-4}	85/15	0.1004
2	0.54	8.0×10^{-4}	20	1	5.70×10^{-5}	1.05×10^{-4}	84/16	0.0982
3	0.37	8.0×10^{-4}	20	1	4.71×10^{-5}	1.28×10^{-4}	85/15	0.1003
4	0.26	8.0×10^{-4}	20	1	3.97×10^{-5}	1.54×10^{-4}	85/15	0.1022
5	0.19	8.0×10^{-4}	20	1	3.29×10^{-5}	1.74×10^{-4}	85/15	0.0997
6	0.54	4.0×10^{-4}	20	1	2.73×10^{-5}	0.51×10^{-4}	84/16	0.0954
7	0.54	12.0×10^{-4}	20	1	8.43×10^{-5}	1.56×10^{-4}	84/16	0.0973
8	0.54	16.0×10^{-4}	20	1	10.91×10^{-5}	2.02×10^{-4}	84/16	0.0945
9	0.54	8.0×10^{-4}	20	2	20.5×10^{-5}	11.5×10^{-4}	72/28	0.0959
10	0.54	8.0×10^{-4}	20	0.5	5.9×10^{-5}	4.42×10^{-4}	85/15	0.1104
11	0.54	8.0×10^{-4}	30	1	5.7×10^{-5}	1.05×10^{-4}	82/18	0.0982
12	0.54	8.0×10^{-4}	10	1	5.8×10^{-5}	1.07×10^{-4}	85/18	0.1001
13	0.54	8.0×10^{-4}	20	3	26.0×10^{-5}	–	–	–

[a] Linear and branched aldehydes are the sole products: ethylbenzene is not detectable.

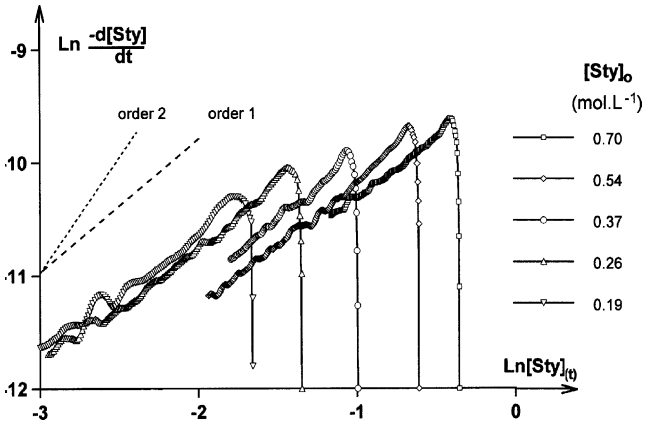

Fig. 4. $\ln(-\mathrm{d}[\mathrm{Sty}]/\mathrm{d}t) = f(\ln[\mathrm{Sty}]_{(t)})$ plot (different styrene concentrations).

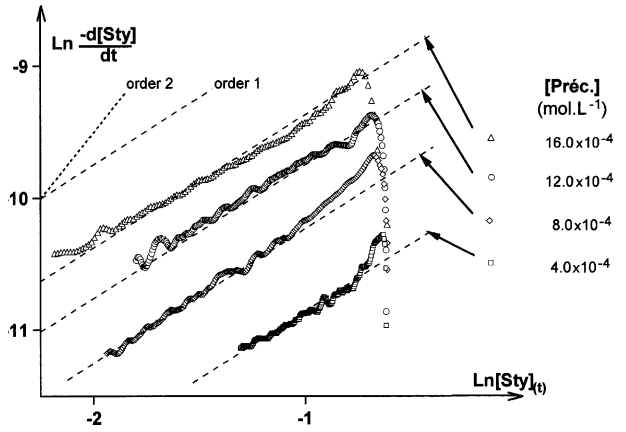

Fig. 5. $\ln(-\mathrm{d}[\mathrm{Sty}]/\mathrm{d}t) = f(\ln[\mathrm{Sty}]_{(t)})$ plot (different catalytic precursor concentrations).

The first is a short duration induction period (about 15 min), corresponding to the formation of the catalytic active species, a homogenization of the reaction mixture and a stabilisation of temperature and pressure. In the second phase, during the steady-state, the reaction rate decreases according to an apparently exponential law. The differential method shows here its efficiency for the reaction progress study: the use of the logarithmic functions discriminates again the representation of weak amplitude phenomena and the use of a unique function, corresponding to a definite and fixed order throughout the reaction, does not allow to put in evidence the possible changes of kinetic regime.

The $\ln R_{(t)} = f(\ln[\mathrm{Sty}]_{(t)})$ plot (Fig. 4) allows determination of the current styrene order. The experimental points, except those situated near the origin of time (when $[\mathrm{Sty}]_{(t)} \approx [\mathrm{Sty}]_0$), fit to different, but parallel straight lines, with slopes corresponding to a current order 1. This graph corresponds to the representation of the equation $\ln R_{(t)} = f(\ln[\mathrm{Sty}]_{(t)}) + B$, where B is a constant (its value depends on the initial substrate concentration). These graphs allowed calculation of the value of the reaction rate, extrapolated at the origin of time (R_0).

2.1.2. Study of the influence of the catalytic precursor concentration (experiments 2, 6, 7, 8)

The $\ln R_{(t)} = f(\ln[\mathrm{Sty}]_{(t)})$ graph (Fig. 5) verifies that, for each of the experiments, the current styrene order is roughly equal to 1. The curves are significantly parallel, which is consistent with an equation of the type:

$$R_{(t)} = -\frac{\mathrm{d}[\mathrm{Sty}]_{(t)}}{\mathrm{d}t} = k_{\mathrm{obs}}[\mathrm{Rh(CO)Cl(TPP)_2}]^1[\mathrm{Sty}]^1_{(t)}$$

$$\text{and consequently :} \quad \ln R_{(t)} = \ln k_{\mathrm{obs}} + \ln(a[\mathrm{Prec_1}]^1) + \ln[\mathrm{Sty}]_{(t)}$$

where $[\mathrm{Prec_1}]$ represents the lowest catalytic precursor concentration ($4.0 \times 10^{-4}\,\mathrm{mol\,L^{-1}}$) and a the multiplicative factor (1, 2, 3 or 4 depending on the experiments). The reactions 2, 6, 7 and 8 were carried out with the same initial styrene concentration so, the $\ln R_{(t)}$ chart values differs from the value $\ln a$ (respectively 0, 0.7, 1.1 and 1.4). The distance to the reference curve ($[\mathrm{Prec_1}] = 4.0 \times 10^{-4}\,\mathrm{mol\,L^{-1}}$) varies according to the $\ln a$ value. We can see that the locations of the experimental curves (Fig. 5) are in full agreement with this hypothesis.

2.1.3. Study of the influence of the total pressure ($pH_2/pCO = 1$) (experiments 2, 11 and 12)

In the catalytic experimental conditions, the partial pressures $p\mathrm{H_2}$ and pCO are equal in the gas phase but the concentrations of these two gases are very different in solution (Table 2).

Their solubility was estimated, using the coefficients of Henry's law in toluene, supplied by Bhanage et al. [38]. This solubility is about $5.9 \times 10^{-3}\,\mathrm{mol\,L^{-1}\,bar^{-1}}$ for CO and $1.8 \times 10^{-3}\,\mathrm{mol\,L^{-1}\,bar^{-1}}$ for $\mathrm{H_2}$, at 323 K.

To study the influence of the total pressure synthesis gas on the reaction rate and on the aldehydes yield, we carried out three experiments (2, 11 and 12) with a total pressure of 10, 20 and 30 bar (all the other conditions being identical to those of the experiment 2). The graph of Fig. 6 represents the styrene disappearance rate with time.

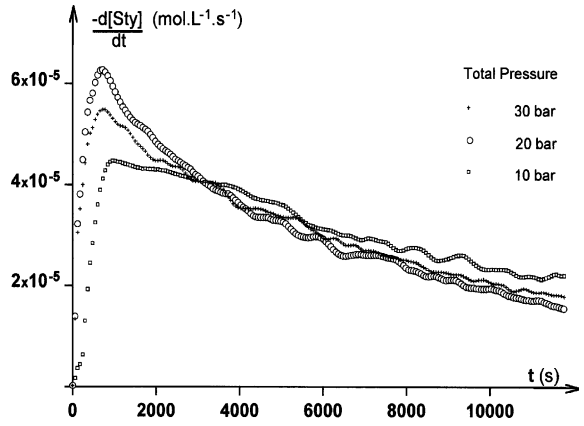

Fig. 6. Total pressure influence on the reaction rate vs. time.

Table 2
Study of the influence of the total pressure and the CO/H_2 ratio

Run	pH_2 (bar)	$[H_2]$ (mol L^{-1})	pCO (bar)	[CO] (mol L^{-1})	pH_2/pCO	$[H_2]/[CO]$	Branched/linear[a]	k_{obs} (s^{-1})	$R_{(t)}$ max (mol L^{-1} s^{-1})
2	10	1.8×10^{-2}	10	5.9×10^{-2}	1	0.30	84/16	1.05×10^{-4}	6.25×10^{-5}
9	14	2.5×10^{-2}	7	4.1×10^{-2}	2	0.60	72/18	–	increasing
10	7	1.2×10^{-2}	14	8.3×10^{-2}	0.5	0.15	85/15	–	0.28×10^{-5}
11	15	2.7×10^{-2}	15	8.8×10^{-2}	1	0.30	84/16	0.95×10^{-4}	5.46×10^{-5}
12	5	0.9×10^{-2}	5	2.9×10^{-2}	1	0.30	82/18	0.72×10^{-4}	4.45×10^{-5}
13	15	2.7×10^{-2}	5	2.9×10^{-2}	3	0.93	–	–	26.0×10^{-5}

$R_{(t)}$max = maximal rate reached at the beginning of the reaction.
[a] Linear and branched aldehydes are the sole products: ethylbenzene is not detectable).

We can see that these curves are not superimposable:

- The maximal rate ($R_{(t)}$max) reached for every experiment is appreciably different.
- The analysis of the curves rate versus time of the styrene concentration (not represented) leads to the determination of different rate constant k_{obs}.
- The linear and branched aldehyde ratio changes slightly when the total pressure increases, as previously observed by Réau [29] in the case of the hexene hydroformylation. In the case of the styrene hydroformylation, the branched aldehyde proportion decreases slightly when the synthesis gas pressure increases.
- The conditions of the reaction seem to be optimal ($R_{(t)}$max and k_{obs}), when the synthesis gas pressure is 20 bar.

These observations reveal the complex role of H_2 and CO in the progress of the reaction.

2.1.4. Study of the influence of the CO/H_2 ratio (experiments 2, 9, 10 and 13)

The graph presented Fig. 7 represents the styrene disappearance rate versus time, for pH_2/pCO's ratio within the range 0.5–3.

The curves were recorded over a 45 min period, but the significance of the results can be discussed in terms of a longer period in the case of a non equimolecular CO/H_2 mixture. Indeed, under such conditions, the gas phase volume is relatively small compared to the volume of the solution. The gas phase thus becomes richer in excess gas during the catalysis and this can modify the steps of the catalytic cycle. This hypothesis is confirmed by the extremely different curve profiles obtained according to the composition of the synthesis gas. Despite the disparity of the experimental conditions and the complexity of the observations, the results of Table 2 allow comparing experiments. Under similar CO concentrations (8.3×10^{-2} and 8.8×10^{-2} mol L^{-1}), the comparison of experiments 10 and 11 shows that the global reaction rate grows when the concentration of H_2 increases (from 1.2×10^{-2} to 2.7×10^{-2} mol L^{-1}). On the reverse, the experiments 13 and 11 demonstrate that with equal concentration of H_2 (2.7×10^{-2} mol L^{-1}), the global reaction rate decreases, when the concentration of CO increases (from 2.9×10^{-2} to 8.8×10^{-2} mol L^{-1}).

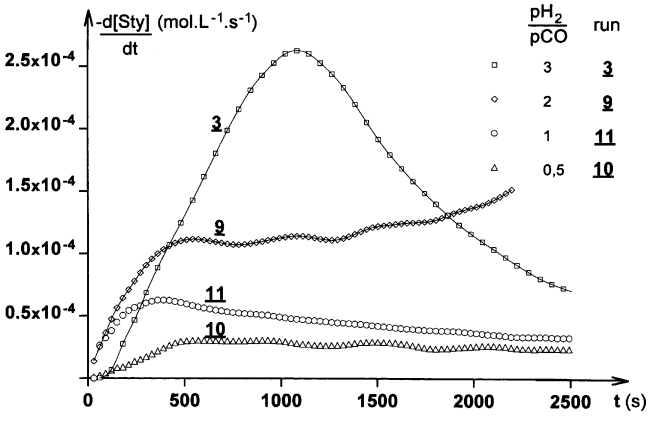

Fig. 7. (pH_2/pCO) ratio influence on the reaction rate.

2.1.5. Study of the influence of the successive additions of styrene

The experimental protocol is as follow: a reaction is carried out under catalytic conditions with a known quantity of styrene. When nearing completion, a quantity of styrene equal to that consumed is added with a high pressure pump (without depressurisation of the reaction mixture). This is repeated when the second reaction nears completion and the reaction is conducted to the end.

The variation of the reaction rate versus time during the successive additions of styrene in the same reaction mixture is shown Fig. 8.

Although the operating mode does not allow the successive reactions to be carried out strictly under the same experimental conditions (uncertainty about the initial styrene consumption; the decrease in reaction mixture temperature after every addition; the solution volume increase), the curves obtained clearly present a different shape. The initial rate strongly decreases for each addition and during the successive styrene additions. Unlike in the first experiment, the curve representing the rate versus time does not decrease in a continuous exponential way, but goes through a maximum. These observations suggested a deactivation of the catalyst, due to the increase of the concentration of aldehydes, and this was corroborated by a reaction carried out in the presence of aldehydes. This inhibitive effect is

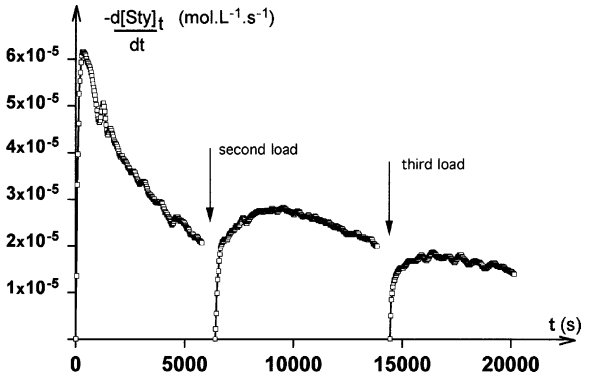

Fig. 8. successive loads of styrene during the hydroformylation reaction (the initial conditions are the same as those of experiment 2 (Table 1).

rarely mentioned in the literature, with most authors conducting the kinetic measurements over a short duration period at the beginning of the reaction. However, Strohmeier and Michel [27] observed this inhibitive effect during the kinetic study of the hex-1-ene hydroformylation in the presence of $HRhCO(PPh_3)_3$. Matsumoto and Tamura [39] too mentioned an inhibitive effect of the reaction products during the oct-1-ene hydroformylation in the presence of the $HRhCO(PPh_3)_3$ catalyst and attributed it to a competition between the aldehyde carbonyl group and the olefin for coordination to the rhodium atom. More recently, van Leeuwen and co-workers [40] observed the deactivation of the hydroformylation catalyst caused by unsaturated ketones, the most likely impurities in alkene feeds. When a reaction was carried out under argon with $HRh(CO)(PPh_3)_3$ and 3-buten-2-one, two η^1-oxygen bound rhodium enolates were characterised. Under CO, these complexes led to inactive carboalkoxyrhodium complexes and under H_2 the hydroformylation catalyst was recovered.

2.2. Proposition of a kinetic equation model

The preceding observations have been completed by spectroscopic studies, useful to build a kinetic equation model. NMR studies of the reaction mixture, when the synthesis gas is a D_2/CO mixture [see footnote 1], give useful information on the mechanism of the first steps of the catalytic cycle, in particular the formation of olefin–rhodium and alkyl-rhodium complexes. During the catalysis reaction, the ^1H and ^2H resonances of the styrene reveal the replacement of one or more hydrogens by deuterium on all sites of the carbon–carbon double bond. This substitution occurs during the reversible formation of the alkyl-rhodium complexes (linear and branched), contrary to what was observed for the other rhodium systems [22,41] where the styrene insertion is irreversible.

The existence of this equilibrium allows us to envisage a reaction mechanism model based on the reversible formation of an association complex. The study of such a type of association complex with transition metal has been widely developed to understand ligand–metal interactions. These interactions concern very different reactions such as the formation of ion pairs [42] of metal complexes [43–45], the oxydo-reduction reactions [45–48] and the various steps of the reactions catalysed by metal complexes [48–52].

Although these studies are relatively new, one can assume that they were widely inspired by those made at the beginning of the 20th century, by Henri [53] and Michaelis and Menten [54]. Indeed, these authors used the association complex model to explain the mechanism of the chemical reactions catalysed by enzymes in solution. The simplified reaction scheme, for the complex of association enzyme–substrate (noted {E–S}), is:

$$\text{Enzyme} + \text{S} \underset{k_{-1}}{\overset{k_1}{\rightleftarrows}} \{\text{E–S}\} \xrightarrow{k_2} \text{Enzyme} + \text{P}$$

The definitive mathematical model was formed by Michaelis and Menten [54]. It was generalised by Briggs and Haldane [55], supposing that all the implied reactions were reversible, involving the free enzyme (E) and possibly several substrates (S), creating several association complexes ({E–S}/{E–P}) and several products (P). The simplified reaction is:

$$\text{E} + \text{S} \overset{\text{reaction (1)}}{\rightleftarrows} \{\text{E–S}\}/\{\text{E–P}\} \overset{\text{reaction (2)}}{\rightleftarrows} \text{E} + \text{P}$$

In the case of the hydroformylation of styrene in the presence of the Rh/TPP system, this model is not directly useful for several reasons:

- The last step of the mechanism namely the hydrogenolysis symbolised here by reaction (2), is irreversible [see footnote 1].
- It is necessary to consider the inhibitive effect of aldehydes. Any mechanism scheme must involve a reversible reaction between aldehydes and an active species in the catalytic cycle (competitive inhibition, according to Cleland's classification [56]). This association complex will be written {C–P}.
- The association complexes ({E–S} and {E–P}) will be written {C–X}, without clarifying if it is about alkyl-rhodium or acyl-rhodium complex, as the reversibility of the formation of acyl-rhodium complex has not been demonstrated [see footnote 1].
- The catalyst exists in the solution, as free (C_L), and in the various association complexes ({C–X}) and aldehydes ({C–P}) at the same time.

These particular hydroformylation conditions lead us to propose the following simplified model:

$$\text{C}_\text{L} + \text{Sty} \underset{k_{-1}}{\overset{k_1}{\rightleftarrows}} \{\text{C–X}\} \xrightarrow{k_2} \text{C}_\text{L} + \text{P} \underset{k_{-3}}{\overset{k_3}{\rightleftarrows}} \{\text{C–P}\} \qquad \text{(R1)}$$

We note that all the reactions parameters are not included in this model: in particular, CO and H_2, although these two species are essential for the catalytic cycle. As the total pressure of the synthesis gas is maintained constant during the experiment, both gases operate in an equimolar mixture and

are consumed in equal quantity. Therefore, partial pressure gases are included in the constant terms of the reaction rate constants.

2.2.1. Reaction study near zero time ($t = 0$)

The mathematical equations of this model (R1) use the hypothesis of the steady-state approximation (Bodenstein approximation) [57,58].

At the beginning of the reaction, the products are in negligible quantities ($[P]_{(t\approx0)} \approx 0$), and the styrene concentration is very similar to the initial one ($[Sty]_{(t=0)} \approx [Sty]_0$).

Thus, reaction scheme R1 can be written:

$$C_L + Sty \underset{k_{-1}}{\overset{k_1}{\rightleftarrows}} \{C\text{–}X\} \xrightarrow{k_2} C_L + P \qquad (R2)$$

The catalyst mass balance expression is:

$$[C_T] = [\{C\text{–}X\}] + [C_L]$$

By applying the steady-state approximation to complex $\{C\text{–}X\}$, we can calculate the expression of the initial reaction rate:

$$R_{(t=0)} = R_0 = -\frac{d[Sty]}{dt} = \frac{k_2[C_T][Sty]_0}{K_M + [Sty]_0} \quad \text{with}$$

$$K_M = \frac{k_{-1} + k_2}{k_1}$$

In this model, the representative curve of the initial rate R_0 versus the initial styrene concentration $[Sty]_0$ is a hyperbola rectangular branch. The determination of the values of constants K_M and $k_2[C_T]$ can be made by various linear methods, among which we have retained the Lineweaver and Burk method [59]. It consists of representing the reciprocal rate extrapolated to time $t = 0$ (noted R_0), versus the initial styrene quantity $[Sty]_0$, which leads to the linear relation:

$$\frac{1}{R_0} = \frac{1}{k_2[C_T]} + \frac{K_M}{k_2[C_T]}\frac{1}{[Sty]_0}$$

The origin ordinate of the obtained straight line is equal to the reciprocal maximal rate to be reached ($R_{max} = k_2[C_T]$) when the catalyst is totally transformed into the complex $\{C\text{–}X\}$, and its slope allows calculation of the value of K_M (Michaelis constant). Our experimental points are significantly aligned with this plot (Fig. 9) and a linear regression allows calculation of K_M (0.39 mol L^{-1}) and R_{max} (0.987×10^{-4} mol L^{-1} s^{-1}).

These two values were used to calculate the branch of a hyperbola which offers the best fit with the experimental points presented in Fig. 10.

This result confirms a Michaelis–Menten type of kinetics. We note that O'Connor and Wilkinson have observed a similarly curve in the hydrogenation of the terminal alkenes in the presence of $HRhCO(PPh_3)_3$ [60], but they have not mentioned the analogy with a Michaelis–Menten type of kinetics.

In our preliminary kinetic study [34], the curve $\ln(k_{1obs}) = f(\ln[Sty]_0)$ looked like a straight line, and this allowed us

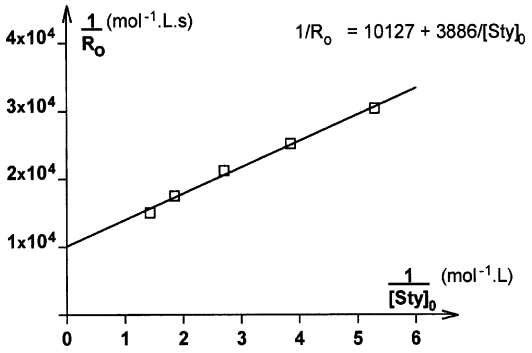

Fig. 9. Lineweaver and Burk plot: $1/R_{(t)} = 1/k_2[C_T] + [(K_M/k_2[C_T])(1/[Sty]_{(t)})]$.

to determine a fractional initial order for the styrene. However, by including the value $R_0 = 0$ for $[Sty]_0 = 0$, the curve obtained can be compared to a hyperbola branch. Therefore, the reaction rate increases according to the substrate initial quantity but tends to an asymptotic value (Fig. 10). This new representation, using the rate equation:

$$R_{(t=0)} = \frac{k_2[Prec]}{K_M + [Sty]_0}[Sty]_0 = k_{1obs}[Sty]_0$$

allows calculation of the values of k_{1obs} and comparison with the previously determined values (Table 3), giving good agreement.

2.2.2. Study of the reaction evolution with time

The assumption of the steady-state approximation to the intermediary species $\{C\text{–}X\}$ is:

$$k_{-1}[\{C\text{–}X\}] + k_2[\{C\text{–}X\}] - k_1[C_L][Sty]_{(t)} = 0$$

$$\frac{[C_L][Sty]_{(t)}}{[\{C\text{–}X\}]} = \frac{k_{-1} + k_2}{k_1} = K_M \quad \text{and}$$

$$[\{C\text{–}X\}] = \frac{1}{K_M}[C_L][Sty]_{(t)}$$

Regarding the inhibition reaction (constants k_3 and k_{-3}), we have the equilibrium constant:

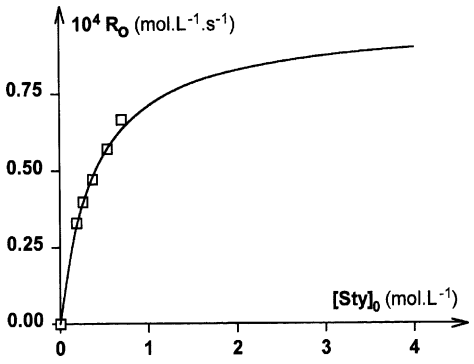

Fig. 10. Initial rate vs. initial styrene concentrations.

Table 3
Experimental and calculated values of k_{1obs} constant vs. styrene concentration

[Styrene] (mol L^{-1})	0.70	0.54	0.37	0.26	0.19
k_{obs} (experimental) (s^{-1})	0.95×10^{-4}	1.05×10^{-4}	1.28×10^{-4}	1.54×10^{-4}	1.74×10^{-4}
k_{1obs} (calculated) (s^{-1})	0.93×10^{-4}	1.08×10^{-4}	1.33×10^{-4}	1.56×10^{-4}	1.75×10^{-4}

$$K_3 = \frac{k_3}{k_{-3}} = \frac{[\{C\text{–}P\}]}{[C_L][P]_{(t)}}, \quad \text{where} \quad [\{C\text{–}P\}] = K_3[C_L][P]_{(t)}$$

The mass balance expression for the catalyst is:

$$[C_T] = [C_L] + [\{C\text{–}X\}] + [\{C\text{–}P\}] = [C_L] + \frac{1}{K_M}[C_L][Sty]_{(t)} + K_3[C_L][P]_{(t)}$$

where

$$[C_L] = [C_T]\frac{1}{1 + (1/K_M[Sty]_{(t)}) + K_3[P]_{(t)}}$$

and the expression of the reaction rate versus time:

$$R_{(t)} = \frac{k_2}{K_M}[C_T]\frac{[Sty]_{(t)}}{1 + (1/K_M[Sty]_{(t)}) + K_3[P]_{(t)}} \quad \text{(E1)}$$

The mass balance expression for the styrene is:

$$[Sty]_0 = [Sty]_{(t)} + [\{C\text{–}X\}] + [\{C\text{–}P\}] + [P]_{(t)}$$

In the conditions of the catalysis, the concentration of the styrene is bigger than that of the catalyst (>300 times), which allows: $[P]_{(t)} \approx [Sty]_0 - [Sty]_{(t)}$ and the expression of the reaction rate versus time:

$$R_{(t)} = \frac{k_2}{K_M}[C_T]\frac{[Sty]_{(t)}}{1 + K_3[Sty]_0 + [Sty]_{(t)}(1/K_M) - K_3} \quad \text{(E2)}$$

To verify the agreement between the experimental and modelled curves (Eq. (E2)), it is necessary to determine the value of the terms $[C_T]$, k_2 and K_3.

The real catalyst concentration is taken as equal to the catalytic precursor concentration ($[C_T] = [Prec]$), as the reaction rate is directly proportional to the initial precursor quantity [34]. This hypothesis is validated by the results of the NMR and IR studies of the reaction mixture prepared from the chlorinated precursor $RhCl(CO)(TPP)_2$ [37,10]. The formation of the catalytic mixture is done in two steps.

A first total reaction, with triethylamine and synthesis gas (pH_2/pCO; 1/1), transforms the precursor $RhCl(CO)(TPP)_2$ into the complex $HRh(CO)_2(TPP)_2$:

$$RhCl(CO)(TPP)_2 + Et_3N + H_2 + CO \xrightarrow[\text{reaction}]{\text{full}} \underset{\text{(H–Rh)}}{HRh(CO)_2(TPP)_2} + Et_3NH^+ + Cl^- \quad \text{(R3)}$$

The complex $HRh(CO)_2(TPP)_2$ is involved in a first equilibrium with TPP, CO, H_2 and a only one dinuclear compound $Rh2(\mu\text{-}CO)_2(CO)_4(TPP)_2$ [see footnote 1]

$$\underset{\text{H–Rh}}{2HRh(CO)_2(TPP)_2} + 2CO \rightleftarrows \underset{\text{(dinuc)}}{Rh_2(\mu\text{-}CO)_2(CO)_4(TPP)_2} + 2TPP + H_2 \quad \text{(R4)}$$

and a second equilibrium with the unsaturated $16e^-$ species $HRh(CO)(TPP)_2$ [see footnote 1]:

$$HRh(CO)_2(TPP)_2 \rightleftarrows HRh(CO)(TPP)_2 + CO \quad \text{(R5)}$$

In the catalysis conditions (with a very large excess of styrene), the influence of the catalyst in the reaction moves the equilibrium R5 to the right and the equilibrium R4 to the left. Thus, the binuclear complexes are almost absent from the reaction mixture [see footnote 1].

Using the values of K_M (0.39 mol L^{-1}) and R_{max} (0.987×10^{-4} mol L^{-1} s^{-1}), we can calculate the constant k_2:

$$\frac{k_2}{K_M} = \frac{R_{max}}{[C_T]K_M} = 0.316, \quad \text{where} \quad k_2 = 0.123$$

We can calculate the term K_3 in the equation E2 using some points chosen during the steady-state reaction. The value varies according to the selected points and the value $K_3 = 2.7$ was chosen because it gives the best fit between the experimental and theoretical curves (Figs. 11 and 12).

By replacing the terms $[C_T]$, k_2 and K_3 and K_M by their numerical value, Eq. (E2) for all the experiments carried out under constant pressure ($pCO = pH_2$) is:

$$R_{(t)} = [Prec]\frac{0.316[Sty]_{(t)}}{1 + 2.7[Sty]_0 - 0.14[Sty]_{(t)}} \quad \text{(E3)}$$

The plotted graphs, overlay of the theoretical curves (Eq. (E3)) and experimental curves, allows validation of the proposed model. This equation shows a hyperbolic

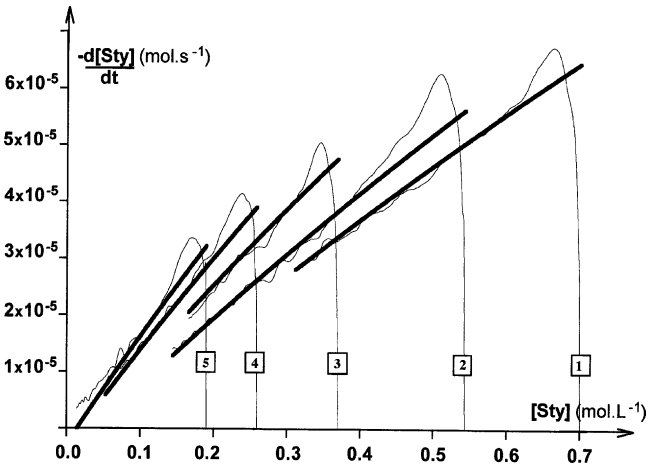

Fig. 11. Plot overlay of experimental and calculated curves (different initial styrene concentrations) (experiments 1–5; Table 1).

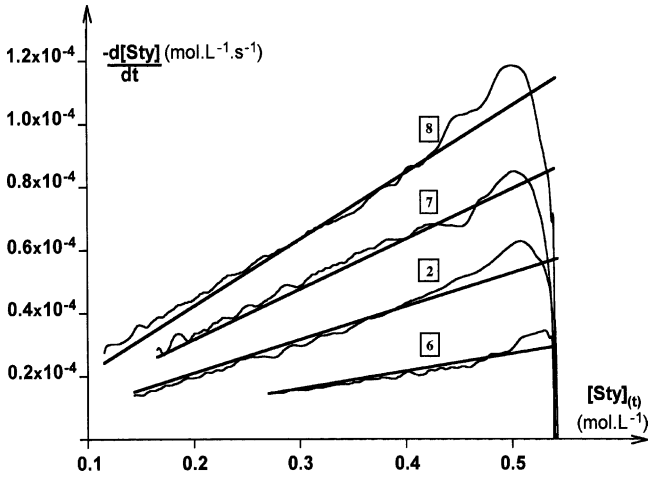

Fig. 12. Plot overlay of experimental and calculated curves (different initial catalytic precursor concentrations) (experiments 6, 2, 7 and 8; Table 1).

behaviour of the reaction rate versus the current styrene concentration. The concavity being weak, this detail was overlooked in our preliminary kinetic studies, and led us to believe in a linear dependence of the rate with the styrene concentration (current order 1). However, this equation confirms the order 1 toward the concentration of the catalyst.

Even though the model of the kinetic Eq. (E3) seems satisfactory, the constant coefficients determined from the experimental results (vide supra) do not allow to establish correlation with the rate constants of the elementary steps of the reaction mechanism. Furthermore, all the experimental parameters susceptible to influence the reaction kinetic were not taken into account: for example, H_2 and CO's participation in some steps of the catalytic cycle and the two ways leading separately to the formation of the linear and branched aldehydes.

2.2.3. Study of the evolution of aldehydes ratio with experimental conditions

All the hex-1-ene hydroformylation studies performed by Réau [29] on styrene hydroformylation (Table 1), show that the ratio of linear/branched aldehydes is independent of the styrene concentration, the catalytic precursor concentration, and the extend of reaction ξ. However, the aldehydes ratio seems to change slightly when the total pressure of synthesis gas varies (CO/H_2; 1/1) and when the synthesis gas is not an equimolar mixture of CO/H_2.

To study the influence of the various experimental parameters, we are now considering that the linear and branched aldehydes formation occurs according to two different and parallel reactions:

$$C_L + Sty \underset{k_{-1Lin}}{\overset{k_{1Lin}}{\rightleftarrows}} \{C\text{–}X_{Lin}\} \xrightarrow{k_{2Lin}} C_L + P_{Lin} \overset{K_{3Lin}}{\rightleftarrows} [C\text{–}P_{Lin}]$$

$$C_L + Sty \underset{k_{-1Ram}}{\overset{k_{1Ram}}{\rightleftarrows}} \{C\text{–}X_{Ram}\} \xrightarrow{k_{2Ram}} C_L + P_{Ram} \overset{K_{3Ram}}{\rightleftarrows} [C\text{–}P_{Ram}]$$

The global rate of the reaction is:

$$R_{(t)} = \frac{d[P_{Ram}]_{(t)}}{dt} + \frac{d[P_{Lin}]_{(t)}}{dt} = k_{2Ram}[\{C\text{–}X_{Ram}\}] + k_{2Lin}[\{C\text{–}X_{Lin}\}]$$

At anytime, whatever the extend of reaction ($\xi_{(t)}$) is, we have also:

$$[\{C\text{–}X\}] = [\{C\text{–}X_{Ram}\}] + [\{C\text{–}X_{Lin}\}]$$

$$[P_{Ram}]_{(t)} = \alpha[P_{Lin}]_{(t)} \quad \text{with} \quad \alpha = \text{constant}$$

$$K_{3Lin} = \frac{k_{3Lin}}{k_{-3Lin}} = \frac{[\{C\text{–}P_{Lin}\}]}{[C_L][P_{Lin}]_{(t)}} \quad \text{and}$$

$$K_{3Ram} = \frac{k_{3Ram}}{k_{-3Ram}} = \frac{[\{C\text{–}P_{Ram}\}]}{[C_L][P_{Ram}]_{(t)}}$$

By applying the steady-state approximation to species $\{C\text{–}X_{Ram}\}$ and $\{C\text{–}X_{Lin}\}$, we can write separately for each complex that the rate of formation and disappearance are:

$$k_{1Ram}[C_L][Sty]_{(t)} = (k_{-1Ram} + k_{2Ram})[\{C\text{–}X_{Ram}\}]$$

$$k_{1Lin}[C_L][Sty]_{(t)} = (k_{-1Lin} + k_{2Lin})[\{C\text{–}X_{Lin}\}]$$

which leads to:

$$[\{C\text{–}X_{Ram}\}] = \frac{[C_L][Sty]_{(t)}}{K_{MRam}}; \quad [\{C\text{–}X_{Lin}\}] = \frac{[C_L][Sty]_{(t)}}{K_{MLin}}$$

with

$$K_{MLin} = \frac{k_{-1Lin} + k_{2Lin}}{k_{1Lin}} \quad \text{and} \quad K_{MRam} = \frac{k_{-1Ram} + k_{2Ram}}{k_{1Ram}}$$

The catalyst mass balance is:

$$[C_T] = [C_L] + [\{C\text{–}X_{Lin}\}] + [\{C\text{–}X_{Ram}\}] + [\{C\text{–}P_{Lin}\}] + [\{C\text{–}P_{Ram}\}]$$

and

$$[C_T] = [C_L]\left(1 + \left(\frac{1}{K_{MRam}} + \frac{1}{K_{MLin}}\right)[Sty]_{(t)} + K_{3Lin}[P_{Lin}]_{(t)} + K_{3Ram}[P_{Ram}]_{(t)}\right)$$

The general expression of the rate constant becomes:

$$R_{(t)} = \left(\frac{k_{2Ram}}{K_{MRam}} + \frac{k_{2Lin}}{K_{MLin}}\right)[C_T][Sty]_{(t)} / \left(1 + \left(\frac{1}{K_{MRam}} + \frac{1}{K_{MLin}}\right)[Sty]_{(t)} + K_{3Lin}[P_{Lin}]_{(t)} + K_{3Ram}[P_{Ram}]_{(t)}\right)$$

The identification of this relation with E1 gives the following expressions:

$$\frac{1}{K_{MRam}} + \frac{1}{K_{MLin}} = \frac{1}{K_M}; \quad k_{2Ram} = k_{2Lin} = k_2 \quad \text{and} \quad K_{3Ram} = K_{3Lin} = K_3$$

The mechanism scheme can be written:

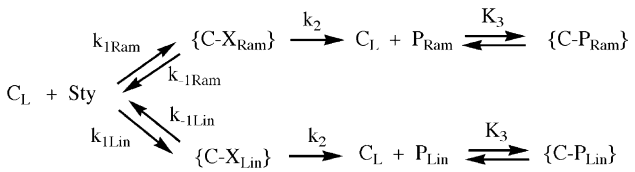

The detailed analysis of this scheme, only established on kinetic considerations, raises several remarks:

- The two parallel reactions, characterised by the rate constants k_{1Lin}, k_{-1Lin}, k_{1Ram} and k_{-1Ram}, implicate the styrene, the catalyst and the linear and branched alkyl-rhodium complexes (vide supra). As the temperature and the extend of reaction have no considerable influence on the aldehydes ratio, we can presume that this first step of the catalytic cycle is not kinetically controlled, but rather thermodynamically controlled. These two parallel reactions have to be considered as two fast thermodynamic equilibria between intermediate complexes $\{C–X_{Lin}\}$, $\{C–X_{Ram}\}$ and the reactants.

  Thus, we can write:

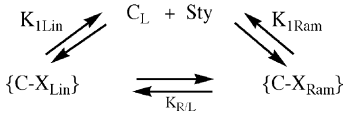

and the thermodynamic constants:

$$K_{1Lin} = \frac{k_{1Lin}}{k_{-1Lin}} = \frac{[\{C–X_{Lin}\}]}{[C_L][Sty]}$$

$$\text{and} \quad K_{1Ram} = \frac{k_{1Ram}}{k_{-1Ram}} = \frac{[\{C–X_{Ram}\}]}{[C_L][Sty]}$$

Thus, we calculate: $[\{C–X_{Lin}\}] = K_{1Lin}[C_L][Sty]$ and $[\{C–X_{Ram}\}] = K_{1Ram}[C_L][Sty]$.

And at every moment: $[\{C–X\}] = [\{C–X_{Lin}\}] + [\{C–X_{Ram}\}] = (K_{1Lin} + K_{1Ram})[C_L][Sty]$.

This allows connecting the thermodynamic constants K_{1Lin} and K_{1Ram} with the constants k_1 and k_{-1} (relation R1):

$$(K_{1Lin} + K_{1Ram}) = \frac{k_1}{k_{-1}}$$

However, we also have:

$$K_{R/L} = \frac{[\{C–X_{Ram}\}]}{[\{C–X_{Lin}\}]} = \frac{K_{1Ram}}{K_{1Lin}} = \alpha$$

In this case, the standard free reaction enthalpy ($\Delta_r G^\circ$) can be calculated from the relative proportions of both isomers (83% and 17%), at 313 K:

$$\Delta_r G^\circ = -RT \ln K_{R/L} \Rightarrow (\Delta_r G^\circ)_{313\,K} = -4.14\,\text{kJ mol}^{-1}$$

If we examine the evolution of the linear/branched aldehydes ratio versus the temperature, supposing that the $(\Delta_r G^\circ)_{313\,K}$ variation is negligible in the temperature range studied, the proportion of isomers varies by approximately 1% for a temperature range variation of 20°, the accuracy of our measurements.

- The second step, modelled as an irreversible reaction, is characterised by a common rate constant k_2 for the two isomers. This result is consistent with the hydrogenolysis step of the rhodium–carbon bond, when the acyl groups are formed [see footnote 1]. The aromatic core of the acyl group is farther from the TPP's groups than in the case of the alkyl complexes and this strongly reduces the steric and electronic interactions. We can presume that the action of H_2 requires similar energy and kinetic conditions for both isomers.
- The inhibition reaction seems to have similar characteristics for both isomers (same equilibrium constant K_3). This observation is consistent with the hypothesis of an inhibition by complexation of the aldehydes with the unsaturated species $HRh(CO)(TPP)_2$ (vide supra) through the oxygen of the carbonyl group [40].

These observations suggest that the kinetic parameters for the formation of the two aldehydes are very similar, so the influence of the synthesis gas has been studied assuming they are not different.

2.2.4. *Influence of CO and H_2 on the catalytic cycle*

The gas concentrations govern both thermodynamics factors (shift of the equilibrium between species) and kinetic factors (accelerating or slowing down effect in some steps).

The rate Eq. (E2) was established for a constant partial pressures gas ratio, which allowed us to include the dissolved gas concentrations in apparent constants. The studies of influence of the pressure and composition of the synthesis gas is required to determine in which equilibrium and elementary steps CO and H_2 are involved. This allows their concentrations to be included in the expressions of the rate constants or the equilibrium constants.

Fig. 13 represents a possible mechanism based on all the current observations under catalysis conditions and during the IR and NMR studies [see footnote 1].

We concluded that the dihydrogen is involved in:

- the formation of the complex $HRh(CO)_2(TPP)_2$ from the precursor $Rh(CO)Cl(TPP)_2$,
- the equilibrium between the binuclear complexes and the $HRh(CO)_2(TPP)_2$ complex,
- step 7, oxidative addition of H_2 to $Rh(CO)(TPP)_2$ (COR(R,L)) {C–A}, the $16e^-$ unsaturated acyl complexes.

The two first reactions cannot be taken into account during the catalytic cycle (vide supra). The dihydrogen is involved only in the step 7 (oxidative addition) and as the reaction rate increases when H_2's partial pressure grows, the concentration of this gas should appear in the analytical expression of the rate of this step.

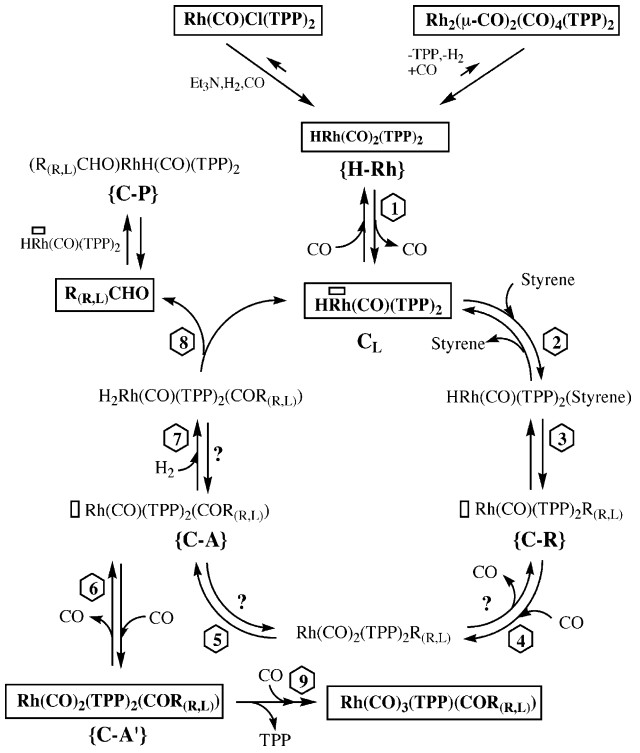

Fig. 13. possible mechanism based on all the observations made in the catalysis conditions and during the IR and NMR studies [see footnote 1].

The carbon monoxide is involved in:

- the formation of the $HRh(CO)_2(TPP)_2$ complex from the precursor $Rh(CO)Cl(TPP)_2$,
- the equilibrium between binuclear and $HRh(CO)_2(TPP)_2$ complexes,
- the equilibrium 1, involving the complex $HRh(CO)_2(TPP)_2$ and the unsaturated species $HRh(CO)(TPP)_2$,
- step 4, coordination on the unsaturated alkyl complexes $Rh(CO)(TPP)_2(R_{(R,L)})$,
- step 6, coordination on the unsaturated acyl species $Rh(CO)(TPP)_2(COR_{(R,L)})$,
- step 9, formation of the $Rh(CO)_3(TPP)(COR_{(R,L)})$ complex, through substitution of one TPP ligand from the complexes $Rh(CO)_2(TPP)_2(COR_{(R,L)})$.

As in the case of H_2, the two first reactions cannot be taken into account in the catalytic cycle (vide supra). Step 9 cannot be considered either in the catalytic cycle, but the $Rh(CO)_3(TPP)(COR_{(R,L)})$ complexes has been detected by NMR studies [see footnote 1]. So, the variations of CO concentration have a complex influence on the catalytic cycle: the increase of its concentration has a positive effect on step 4, but a negative effect on step 1 (decrease of the concentration of the unsaturated species C_L), and step 6 (formation of the inert saturated acyl complexes $\{C–A'\}$).

2.3. General kinetic equation

The introduction of the two gas concentrations in the various steps of the reaction mechanism allows to write a set of reactions, presented in scheme R6, leading to the calculation of a more complete expression of the rate equation:

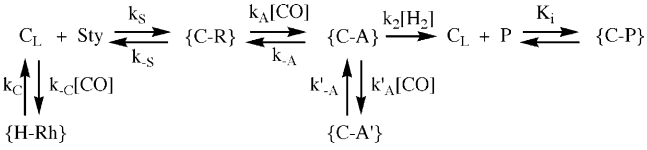

(R6)

By applying the steady-state approximation, we can write for each complex $\{C–R\}$, $\{C–A\}$ and $\{C–A'\}$, that the creation and disappearance rates are the same:

$$\frac{d[\{C–R\}]}{dt} = 0 = k_S[C_L][Sty]_{(t)} + k_{-A}[\{C–A\}] - (k_A[CO + k_{-S})[\{C–R\}]$$

$$\frac{d[\{C–A'\}]}{dt} = 0 = k'_{-A}[\{C–A'\}] - k'_A[CO][\{C–A\}]$$

$$\frac{d[\{C–A\}]}{dt} = 0 = k_A[CO][\{C–R\}] - (k_{-A} + k_2[H_2] + k'_A[CO])[\{C–A\}] + k'_{-A}[\{C–A'\}]$$

$$[\{C–A'\}] = \frac{k'_A[CO][\{C–A\}]}{k'_{-A}}$$

$$[\{C–R\}] = \frac{k_S[C_L][Sty]_{(t)}}{k_{-S} + k_A[CO]} + \frac{k_{-A}[\{C–A\}]}{k_{-S} + k_A[CO]} = \frac{(k_{-A} + k_2[H_2])[\{C–A\}]}{k_A[CO]}$$

$$[\{C–A\}] = [C_L][Sty]_{(t)}\frac{1}{K_M} \quad \text{with}$$

$$K_M = \frac{k_A[CO](k_{-S} + k_A[CO])}{k_S(k_{-A} + k_2[H_2])} - \frac{k_{-A}}{k_S} \qquad \text{(E4)}$$

$$[H–Rh] = \frac{k_C[C_L][CO]}{k_{-C}}$$

The mass balance catalyst is:

$$[C_T] = [Prec] = [C_L] + [\{C–R\}] + [\{C–A\}] + [\{C–A'\}] + [\{C–P\}] + [H–Rh]$$

Thus:

$$[Prec] = [C_L]\left\{1 + \frac{[Sty]_{(t)}}{K_M}\left(1 + \frac{k_{-A} + k_2[H_2]}{k_A[CO]} + \frac{k'_A[CO]}{k'_{-A}}\right) + \frac{k_C[CO]}{k_{-C}} + K_I[P]\right\}$$

The general expression of the rate becomes:

$$R_{(t)} = k_2[H_2][\{C\text{–}A\}] = \frac{k_2[H_2]}{K_M}[C_L][Sty]_{(t)}$$

$$R_{(t)} = k_2[H_2][Prec][Sty]_{(t)} / \left(K_M \left(1 + K_I[P]s + \frac{k_C[CO]}{k_{-C}} \right) + [Sty]_{(t)} \left(1 + \frac{k_{-A} + k_2[H_2]}{k_A[CO]} + \frac{k'_A[CO]}{k'_{-A}} \right) \right) \quad (E5)$$

This general reaction rate expression reflects the complex influence of the CO and H_2 concentrations. Although most of the constants are unknown, it is possible to do a qualitative analysis, gathering the constant terms and the terms which imply the CO and H_2 concentrations. If the sole variable is the hydrogen concentration, Eq. (E5) has the form:

$$R_{(t)} = \frac{A[H_2]}{C[H_2] + BK_M + D}$$

where A, B, C and D are constant terms.

$[H_2]$ is involved both in the numerator and the denominator and the constant terms A, B, C and D are all positive and the equation determinant ($A(BK_M + D)$) is positive. The plot of this curve ($R_{(t)} = f([H_2])$) is a equilateral hyperbola branch for which $R_{(t)}$ grows with $[H_2]$. In reality, the term K_M is not the same according to the respective values of $[H_2]$ and [CO] (Eq. (E4)), but this does not affect the general aspect of the curve (increasing hyperbola branch). So, we can conclude that the reaction rate grows when the H_2 partial pressure increases.

In the same conditions, if the sole variable is [CO], the expression E5 can be written:

$$R_{(t)} = \frac{A'}{[CO](B'K_M + C') + (D'/[CO]) + E'K_M + F'}$$

where A', B', C', D', E' and F' are constant terms.

Although [CO] is involved only in the denominator, the study of the evolution of the reaction rate is difficult. The terms K_M and $[CO](B'K_M + C')$ increase when [CO] increases (relation E4), while the term $(D'/[CO])$ decreases. So, the evolution of the denominator value will be a function of the relative value of these various terms. The values of constants being unknown, it is difficult for us to predict the evolution of the reaction rate according to [CO].

All these results, concerning the influence of the composition and the total pressure of synthesis gas, are in agreement with our experimental observations: the reaction rate increases with the H_2 concentration in the solution but the increase of the relative CO concentration can have a positive or negative effect (Table 2 and Fig. 7).

This provides insight into the influence of the total pressure on the reaction rate (Fig. 6) and specially the influence of the variation of CO/H_2 partial pressures, when the composition of the synthesis gas varies during the catalytic reaction (Fig. 7). The most representative experiments 9 and 3, were carried out with different [H2]/[CO]'s concentration ratios

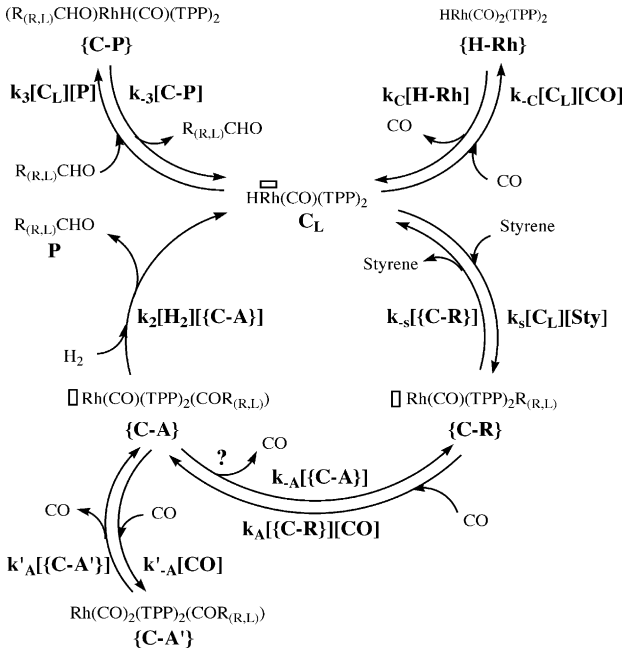

Fig. 14. Scheme of the mechanism reaction associating reaction intermediates with the determining steps of the catalytic cycle.

(respectively, 0.93 and 0.60) (Table 2). This ratio increases in both cases with the progress of the reaction (vide supra). We observe however two curves of very different aspects, experiment 3 gives a "bell" curve and experiment 9 a continuously increasing curve, which provides evidence for the simultaneous effects of the concentrations of both gases. In experiment 9, the accelerating effect of the increase in concentration of H_2 is linked with the decrease in concentration of CO, leading to a continuously increasing curve, despite the decrease in concentration of styrene. In experiment 3, the accelerating effect of the increase of the concentration of H_2 is also linked with the decrease in CO concentration, but the initial concentration of CO is smaller (2.9×10^{-2} mol L^{-1} instead of 4.1×10^{-2} mol L^{-1}) and this leads to a faster growth of the reaction rate. The rate passes then through a maximum and seems to undergo a diminution following a classic exponential.

The analysis of all the experimental results, from the point of view of the detected species and their kinetic behaviour, allows us to propose a scheme of the mechanism reaction associating reaction intermediates with the determining steps of the catalytic cycle (Fig. 14).

The results of the kinetic studies show that it is the formation of three $16e^-$ unsaturated complexes (C_L, {C–R} and {C–A}) and their ability to react with the various ligands (CO, H_2, styrene) which make up the key steps of the mechanism.

The unsaturated complex C_L is the true catalytic species of the reaction. It is involved simultaneously in three reactions: the equilibrium of its creation from the precursor {H–Rh}, the complexation equilibrium with aldehydes, leading to the saturated complexes {C–P} and the equilibrium with the

unsaturated alkyl-rhodium complexes {C–R}. The concentration in the reaction mixture is a function of various experimental parameters: in particular, it decreases with increase in the styrene concentration, CO concentration (step 1, Fig. 13) or aldehydes concentration (inhibitive effect (Fig. 8), increasing with the progress of the reaction).

The two other important unsaturated complexes are the alkyl-rhodium species {C–R}, which are involved in the regeneration of the complex C_L and the formation of the unsaturated acyl-rhodium complexes {C–A}. The formation of these last complexes precedes the step of hydrogenolysis of the rhodium–acyl bond. Therefore, their concentrations are included in the expression of the reaction rate, but it varies according to the CO concentration as they are also involved in the equilibrium with the saturated acyl-rhodium species {C–A′}. This illustrates the inhibitive effect of the increase of the CO concentration, while the increase of the H_2 concentration accelerates the rate of the hydrogenolysis step.

Although this reaction scheme satisfies all the observations and the measurements, there is a point we were not able to clarify: is the creation of acyl-rhodium complex {C–A} a reversible or an irreversible step? What are the kinetic consequences?

The ^{13}C and ^{31}P NMR studies of ^{13}CO enriched reaction mixtures did not allow to answer this question [see footnote 1]. Also, our kinetic study does not bring information in favour of one or other of the possibilities and does not establish the CO's concentration as a kinetic factor in this step: it is possible that the carbonyl group insertion in the rhodium carbon bond (or the migration of the alkyl group) was of order zero or of order 1 (following the CO concentration), as was observed in the case of manganese [61–63]. In our case, we can notice that the irreversibility of the reaction has few consequences on the general kinetic Eq. (E5), as this last reaction is only slightly modified when the constant k_{-A} is zero (this corresponds to an irreversible formation of the acyl-rhodium complexes {C–A}).

3. Conclusion

Our preliminary kinetic study allowed us to propose a global analytical equation, reflecting the most important reactions occurring in the catalytic cycle. This equation, based on the Van't Hoff model, reflected in a rather simple way the kinetic behaviour of the reaction system, but it led to values of partial orders difficult to correlate to a reaction mechanism scheme.

This more complete kinetic study has allowed us to refine the experimental curves and to study more deeply the influence of the reaction parameters.

So, we have been able to propose a model of mechanism with an association complex between $HRh(CO)(TPP)_2$ and the styrene. This model allows an analytical equation of the reaction rate, based on the Michaelis and Menten's model to be established. It satisfactorily characterises the behaviour of the reaction rate according to the concentration of the various species.

The relative proportions of aldehydes do not change significantly with the reaction parameters (extend of reaction, temperature, pressure, synthesis gas composition), which reveals a dependence of the selectivity towards thermodynamic rather than kinetic criteria. The isotopic substitutions observed in the various species (aldehydes, styrene) confirm the existence of thermodynamic equilibrium between the linear and branched alkyl-rhodium species. If the isomeric acyl-rhodium species are also present, it would require the reversibility of the transformation of alkyl-rhodium isomers in acyl-rhodium isomers. Unfortunately, our studies did not allow clarification about the reversibility or the irreversibility of this reaction. The relative constancy of the aldehydes isomers ratio formed in various experimental conditions, demonstrates as well that, except for the differentiation brought by the thermodynamic equilibrium, the synthetic route for linear and branched isomers is appreciably similar, and that the kinetic constants occurring in the various steps have very close values. This can be extended to the value of the complexation equilibrium constants of the aldehydes with the catalyst (inhibitive effect).

The influence of the total pressure and the composition of the synthesis gas on the progress of the catalytic cycle are complex because H_2 and CO concentrations determine the concentration of the reaction intermediates and are required in the kinetics of the various steps. The evident conclusion of these observations is that the influence of the composition of the synthesis gas cannot be summarised, as we proposed in the preliminary study, to the simple ratio of the gases partial pressure in the rate equation.

Finally, we have been able to propose a reaction mechanism consistent with a kinetic equation because the Rh/TPP system is almost an ideal case. Indeed, the catalytic cycle is done with a unique catalyst having two TPP ligands per Rh atom and all the intermediate species involved never undergo the dissociation of a phosphorus ligand. The hydroformylation is characterised by a single catalytic cycle, only differentiated by the creation of the linear and branched aldehydes.

4. Experimental section

4.1. Reagents

All the gases are of high purity (argon U, CON20, N_2U and H_2U of the "L'Air Liquide" company). Before use, all the solvents were dried, distilled and degased according to the literature procedure. They were stored under N_2 or Ar after distillation. The 1,2,5-triphenyl-1*H*-phosphole was supplied by Mathey [64], or prepared according to Lukas et al. [65]. The triethylamine (Janssen Chimica, 99%) was distilled over sodium and kept under argon. The styrene (Fluka, >99%) was distilled over calcium dihydride,

placed under argon, then kept at −30 °C and shielded from the light. Hydratropaldehyde (Acros, 98%) and hydrocinnamaldehyde (Acros, 97%) were distilled under reduced pressure then kept under argon. The catalytic precursor $RhCl(CO)(TPP)_2$ was prepared according to Neibecker and Réau [31], from the di-μ-chloro-tetracarbonyldirhodium $(CO)_2Rh(\mu\text{-}Cl)_2Rh(CO)_2$ [66].

4.2. Hydroformylation experiments

In a typical run, $RhCl(CO)(TPP)_2$ was introduced into the autoclave which was closed, and flushed with argon. A toluene solution containing triethylamine was introduced. The autoclave was pressurized with synthesis gas and heated at the desired temperature for 10 min. Styrene was then injected (the total reaction mixture was 50 mL) and the gas consumption monitored.

4.3. Kinetic study

The experimental apparatus was described in a previous paper [34]. The kinetics were followed by measurement of the synthesis gas absorption versus time, using computer controlled automatic acquisition (several hundred per experiment). A software enabled a complete and rigorous treatment of all the measurements to be conducted. After smoothing by simplified least squares procedures [67] or by the cubic splines [68], the program calculated the quantity of substrate transformed versus time and plotted the corresponding graph. The substrate consumption rate and the rate constant could then be determined.

The experimental conditions of the study and ranges of variation of the parameters were: substrate: styrene (104.16 g mol^{-1}), range 0.19–0.70 mol L^{-1}; catalytic precursor: $RhCl(CO)(TPP)_2$ (791.07 g mol^{-1}), range 4×10^{-4} to 16×10^{-4} mol L^{-1}; ratio [substrate]/[catalytic precursor]: range 238–1350; triethylamine (101.19 g mol^{-1}), range 4×10^{-3} to 16×10^{-3} mol L^{-1}; synthesis gas: H_2/CO; reactor temperature range: 31–60 °C; reactor pressure range: 10–30 bar; agitation speed: 1000 rpm; solvent: toluene; solution bulk: 50 mL.

The results from various experiments are collected in Table 1.

4.4. Chromatographic analysis

Chromatographic analyses by C.P.V. were carried on a Intersmat IGC 120 DFL, equipped with a flame ionisation detector. Quantitative analyses were conducted with the internal standard method.

Standard analysis: At the end the catalytic experiment, the autoclave was cooled quickly towards 5–10 °C (cooling thermostat). After depressurisation, the reaction mixture was collected in a Schlenk tube, under argon, and analyzed by C.P.V. (column: 10% carbowax 20 M on chromosorb 80–100 mesh; sizes: 3 m/1/8″; vector gas: N_2).

4.5. Representative experimental NMR and IR data on complexes

Complex $HRh(CO)_2(TPP)_2$
IR (298 K, CH_2Cl_2, CaF_2, 1 mm): 2050 w(ν Rh–H), 1988s, 1955w;
^{1}H NMR (273 K, CD_2Cl_2): δ −9.92 (td, J(H–P) = 7.5 Hz, J(H–Rh) = 2.0 Hz);
^{31}P NMR (273 K, CD_2Cl_2): δ 35.3 (dm, J(P–Rh) = 130 Hz);
^{13}C NMR (273 K, CD_2Cl_2): δ 198.0 (dm, J(C–Rh) = 63 Hz, J(C–H) = 18 Hz, J(C–P) = 9 Hz).

Complex $Rh2(\mu\text{-}CO)_2(CO)_4(TPP)_2$:
IR (298 K, CH_2Cl_2, CaF_2, 1 mm): 2063w, 2037m, 2016w, 1819w, 1796w;
^{31}P NMR (273 K, CD_2Cl_2): δ 29.5 (d, J(P–Rh) = 138.5 Hz);
^{31}P NMR (173 K, CD_2Cl_2): δ 32.9 (d, J(P–Rh) = 90 Hz, 1P), 24.5 (d, J(P–Rh) = 150 Hz, 1P);
^{13}C NMR (273 K, CD_2Cl_2): δ 203.3 (t, J(C–Rh) = 31 Hz);
^{13}C NMR (173 K, CD_2Cl_2): δ 227.7 (m, 2C), 194.6 (d, J(C–Rh) = 53 Hz, 1C), 191.2 (d, J(C–Rh) = 50 Hz, 1C), 190.3 (d, J(C–Rh) = 90 Hz, 1C), 188.5 (d, J(C–Rh) = 50 Hz, 1C).

Complex $HRh(CO)(TPP)_2$:
IR (298 K, CH_2Cl_2, CaF_2, 1 mm): 1945w.

Complex $Rh(CO)_3(TPP)(COR_{(R)})$ ($R_{(R)}$ = –CH(CH_3)Ph):
^{1}H NMR (193 K, CD_2Cl_2): δ 1.20 (dd, ^3J(H–H) = 6.5 Hz, ^2J(H–C) = 7 Hz, 3H), 4.25 (qd, ^3J(H–H) = 6.5 Hz, ^2J(H–C) = 7 Hz, 1H);
^{31}P NMR (193 K, CD_2Cl_2): δ 34.16 (m, J_1(P–C) = 67 Hz, J_2(P–C) = 15 Hz, J(P–Rh) = 65 Hz);
^{13}C NMR (193 K, CD_2Cl_2): δ 231.0 (dd, J(C–P) = 66 Hz, J(C–Rh) = 19 Hz, 1C(CO acyl)), 189.5 (dd, J(C–P) = 16 Hz, J(C–Rh) = 74 Hz, 3C(CO)).

Complex $Rh(CO)_3(TPP)(COR_{(L)})$ ($R_{(L)}$ = –CH_2–CH_2–Ph):
^{1}H NMR (193 K, CD_2Cl_2): δ 2.65 (m, ^3J(H–H) = 7.5 Hz, ^2J(H–C) = 7 Hz, 2H), 3.15 (m, ^3J(H–H) = 7.5 Hz, ^2J(H–C) = 7 Hz, 2H);
^{31}P NMR (193 K, CD_2Cl_2): δ 34.34 (m, J_1(P–C) = 67 Hz, J_2(P–C) = 15 Hz, J(P–Rh) = 65 Hz);
^{13}C NMR (193 K, CD_2Cl_2): δ 227.3 (dd, J(C–P) = 64 Hz, J(C–Rh) = 18 Hz, 1C(CO acyl)), 190.2 (dd, J(C–P) = 16 Hz, J(C–Rh) = 74 Hz, 3C(CO)).

Complex $Rh(CO)_2(TPP)_2(COR_{(R)})$ ($R_{(R)}$ = –$CH(CH_3)$Ph):
^{1}H NMR (193 K, CD_2Cl_2): δ 1.32 (m, 3H), 4.35 (m, 1H);
^{13}C NMR (193 K, CD_2Cl_2): δ 235.0 (td, J(C–P) = 25 Hz, J(C–Rh) = 25 Hz, 1C(CO acyl)), 187.7 (m, J(C–P) = 10 Hz, J(C–Rh) = 70 Hz, 2C(CO)).

Complex $Rh(CO)_2(TPP)_2(COR_{(L)})$ ($R_{(L)}$ = –CH_2–CH_2–Ph):
^{1}H NMR (193 K, CD_2Cl_2): δ 2.65 (m, 2H), 3.10 (m, 2H).

The ^{1}H, ^{31}P and ^{13}C NMR spectra were recorded at different temperatures on a BRUKER AC200, AM250 or AMX400 spectrometer. Chemical shifts are reported in ppm (δ) relative to solvent proton ($CHDCl_2$: 5.33 ppm) for ^{1}H, H_3PO_4 in D_2O solution (external reference) for ^{31}P and ^{13}C of the solvent (^{13}C D_2Cl_2: 53.6 ppm) for ^{13}C NMR, respectively. The IR spectra were recorded on a FT-IR Perkin-Elmer 1725-X spectrometer.

References

[1] K. Weissermel, H.J. Harpe, Industrial Organic Chemistry, VCH Publishers, New York, 1993.
[2] M. Beller, B. Cornils, C.D. Frohning, C.W. Kohlpaintner, J. Mol. Catal. 104 (1995) 17.
[3] N. Sakai, S. Mano, K. Nozaki, H. Tayaka, J. Am. Chem. Soc. 115 (1993) 7033.
[4] J.K. Stille, in: B.M. Trost, I. Fleming, M.F. Semmelhack (Eds.), Comprehensive Organic Syntheses, vol. 4, Pergamon, Oxford, 1991, p. 913.
[5] P.P. Deutsch, R. Eisenberg, Organometallics 9 (1990) 709.
[6] R. Schmidt, W.A. Herrmann, G. Frenking, Organometallics 16 (1997) 701.
[7] T. Matsubara, N. Koga, Y. Ding, D.G. Musaev, K. Morokuma, Organometallics 16 (1997) 1065.
[8] T.J. Kwok, D.J. Wink, Organometallics 12 (1993) 1954.
[9] G. Consiglio, F. Morandini, P. Haelg, P. Pino, J. Mol. Catal. 60 (1990) 363.
[10] D. Evans, J.A. Osborn, G. Wilkinson, J. Chem. Soc. A (1968) 3133.
[11] R.F. Heck, D.S. Breslow, J. Am. Chem. Soc. 83 (1961) 4023.
[12] C.K. Brown, G. Wilkinson, J. Chem. Soc. A (1970) 2753.
[13] F.H. Jardine, Polyhedron 1 (1982) 569.
[14] J.M. Brown, A.G. Kent, J. Chem. Soc. Perkin Trans. 2 (1987) 1597.
[15] V.S. Nair, S.P. Mathew, R.V. Chaudhari, J. Mol. Catal. 143 (1999) 99.
[16] S.C. van der Slot, P.C.J. Kamer, P.W.N.M. Leeuwen, J.A. Iggo, B.T. Heaton, Organometallics 20 (2001) 430.
[17] I. del Rio, O. Pamies, P.W.N.M. Leeuwen, C. Claver, J. Organometal. Chem. 608 (2000) 115.
[18] W.R. Moser, C.J. Papile, D.A. Brannon, R.A. Duwell, S.J. Weininger, J. Mol. Catal. 41 (1987) 271.
[19] J.D. Unruh, J.R. Christenson, J. Mol. Catal. 14 (1982) 19.
[20] C. Bianchini, A. Meli, M. Peruzzini, F. Vizza, Y. Fujiwara, T. Jintoku, H. Taniguchi, J. Chem. Soc. Chem. Commun. (1988) 299.
[21] T. Jongsma, G. Challa, P.W.N.M. van Leeuwen, J. Org. Chem. 421 (1991) 121.
[22] A. van Rooy, E.N. Orij, P.C.J. Kamer, F. van den Aardweg, P.W.N.M. van Leeuwen, Organometallics 14 (1995) 34.
[23] L.A. van der Veen, M.D.K. Boele, F.R. Bregman, P.C.J. Kamer, P.W.N.M. van Leeuwen, K. Goubitz, J. Fraanje, H. Schenk, C. Bo, J. Am. Chem. Soc. 120 (1998) 11616.
[24] M. Royo, F. Melo, A. Manrique, Trans. Met. Chem. 7 (1982) 44.
[25] R.M. Deshpande, R.V. Chaudhari, Ind. Eng. Chem. Res. 27 (1988) 1996.
[26] P.C. d'Oro, L. Raimondi, G. Pagani, G. Montrasi, G. Gregoro, A. Andreetta, Chim. Ind. (Milan) 62 (1980) 572.
[27] W. Strohmeier, M. Michel, Z. Phys. Chem. 124 (1981) 23.
[28] A. van Rooy, E.N. Orij, P.C.J. Kamer, F. Van den Aardweg, P.W.N.M. Van Leeuwen, J. Chem. Soc., Chem. Commun. 16 (1991) 1096.
[29] R. Réau, Thèse de Doctorat d'Université, Toulouse, 1988.
[30] D. Neibecker, R. Réau, J. Mol. Catal. 53 (1989) 219.
[31] D. Neibecker, R. Réau, J. Mol. Catal. 57 (1989) 153.
[32] D. Neibecker, R. Réau, S. Lecolier, J. Org. Chem. 54 (1989) 5208.
[33] D. Neibecker, R. Réau, New J. Chem 15 (1991) 279.
[34] C. Bergounhou, D. Neibecker, R. Réau, Bull. Soc. Chim. 132 (1995) 815.
[35] C. Bergounhou, D. Neibecker, R. Réau, J. Chem. Soc., Chem. Commun. (1988) 1370.
[36] A. Polo, C. Claver, S. Castillon, A. Ruiz, J.C. Bayon, J. Real, C. Mealli, D. Masi, Organometallics 11 (1992) 3525.
[37] C. Bergounhou, D. Neibecker, R. Mathieu, Organometallics 22 (2003) 782.
[38] B.M. Bhanage, S.S. Divkar, R.M. Deshpande, R.V. Chaudhari, J. Mol. Catal. 115 (1995) 247.
[39] M. Matsumoto, M. Tamura, J. Mol. Catal. 16 (1982) 209.
[40] E.B. Walczuk, P.C.J. Kamer, P.W.N.M. van Leeuwen, Angew. Chem. Int. Ed. 42 (2003) 4665.
[41] G. Ucello-Barretta, R. Lazzaroni, R. Settembolo, P. Salvadori, J. Organomet. Chem. 417 (1991) 111.
[42] F.M. Beringer, E.M. Gindler, J. Am. Chem. Soc. 77 (1955) 3200.
[43] A.D. Attie, R.T. Raines, J. Chem. Ed. 72 (1995) 119 (Ref. [5]).
[44] R.L. Reeves, G.S. Calabrese, S.A. Harkaway, Inorg. Chem. 22 (1983) 3076.
[45] D. Benson, Introduction aux mécanismes des réactions inorganiques en solution, Masson, 1972.
[46] N. Al-Shatti, A.G. Lappin, A.G. Sykes, Inorg. Chem. 20 (1981) 1466.
[47] R.G. Wilkins, Kinetics and Mechanism of Reactions of Transition Metal Complexes, VCH Publishers, New York, 1991.
[48] D. Huchital, R.G. Wilkins, Inorg. Chem. 6 (1967) 1022.
[49] K.A. Connors, Chemical Kinetics, VCH Publishers, New York, 1990 (ISBN 1-56081-006-8).
[50] N. Emanuel, D. Knorre, Cinétique Chimique, Editions MIR, Moscou, 1975.

[51] J.M. Brégeault, Catalyse homogène par les complexes des métaux de transition, Masson, Paris, 1992.
[52] M.T. Ashby, J. Halpern, J. Am. Chem. Soc. 113 (1991) 589.
[53] V. Henri, C. R. Acad. Sci. 135 (1902) 916.
[54] L. Michaelis, M.L. Menten, Biochemistry 49 (1913) 3426.
[55] G.E. Briggs, J.B.S. Haldane, Biochem. J. 19 (1925) 338.
[56] W.W. Cleland, Biochim. Biophys. Acta 67 (1963) 183.
[57] M. Bodenstein, Z. Physik. Chem. 85 (1913) 329.
[58] P.C. Engel, Enzyme Kinetics—The Steady-State Approach, Chapman and Hall, London/New York, 1981.
[59] H. Lineweaver, D. Burk, J. Am. Chem. Soc. 56 (1934) 658.
[60] C. O'Connor, G. Wilkinson, J. Chem. Soc. A (1968) 2665.
[61] R.B. Jordan, Reaction Mechanisms of Inorganic and Organometallic Systems, Oxford University Press, New York, 1998.
[62] F. Calderazzo, Angew. Chem., Int. Ed. Engl. 16 (1977) 299.
[63] H. Berke, R. Hoffmann, J. Am. Chem. Soc. 100 (1978) 7224.
[64] F. Mathey, Chem. Rev. 88 (1988) 429.
[65] B. Lukas, R.M.G. Roberts, J. Silver, A.S. Wells, J. Organomet. Chem. 103 (1983) 256.
[66] J.A. McCleverty, G. Wilkinson, Inorg. Synth. 8 (1966) 211.
[67] A. Savitzky, M.J.E. Golay, Anal. Chem. 36 (1964) 1627.
[68] K. Ebert, H. Ederer, J.L. Isenhour, Computers Applications in Chemistry, VCH Publishers, New York,1989.